Electronic Supplementary Material (ESI) for Soft Matter.

Supplementary information for

Cohesive and adhesive properties of crosslinked semiflexible biopolymer networks

Yao Zhang[1], Elizabeth P. DeBenedictis[1], Sinan Keten[1,2,*]

[1]Department of Mechanical Engineering, Northwestern University, Evanston, Illinois 60208, United States

[2]Department of Civil and Environmental Engineering, Northwestern University, Evanston, IL 60208, United States

[*] Corresponding author

E-mail: s-keten@northwestern.edu

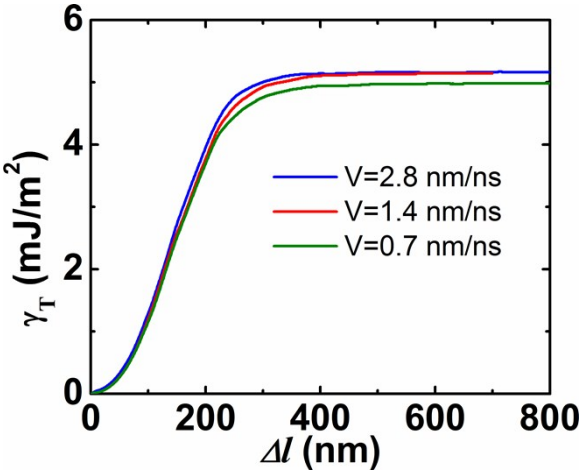

Figure S1. The effect of pulling velocity in SMD on the measured work of adhesion.

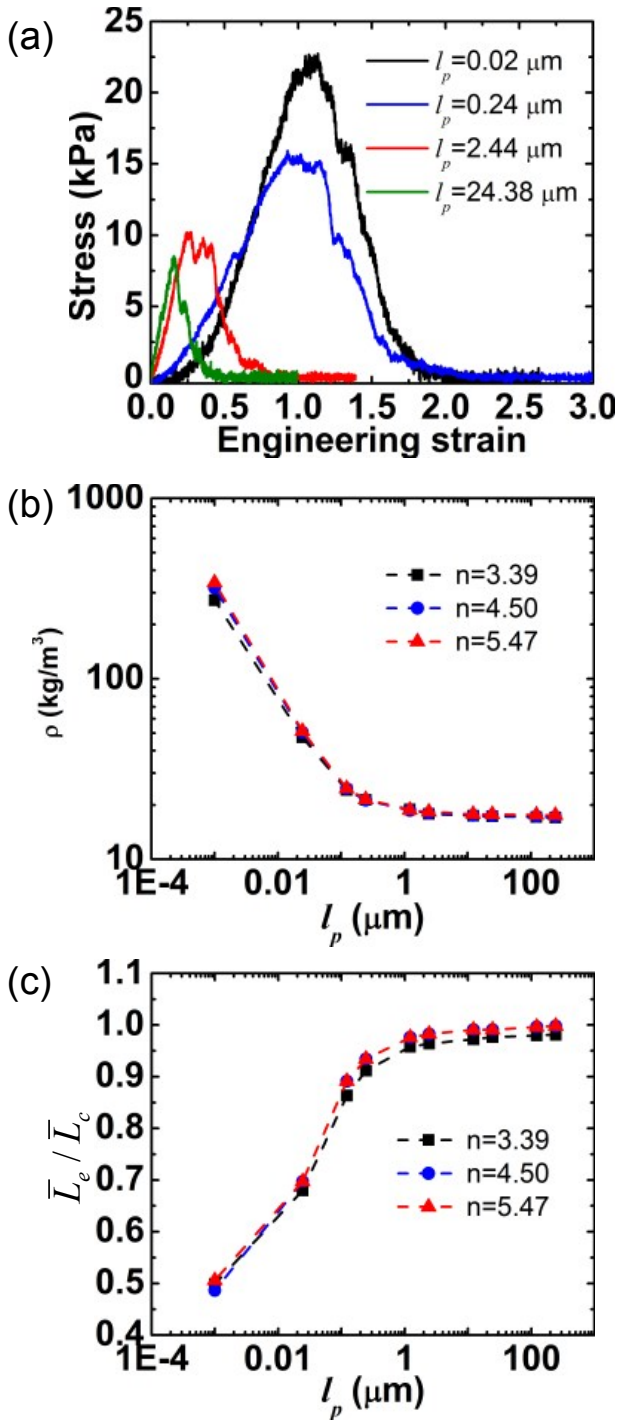

Figure S2. (a) The internal stress and strains generated in networks with different persistence lengths during force-induced detachment (n=4.50); (b) The effect of fibril persistence length on mass density; (c) The ratio of mean end-to-end distance ($\bar{L}_e$) to the corresponding mean contour length ($\bar{L}_c$) of fibril segments in networks as a function of fibril persistence length.

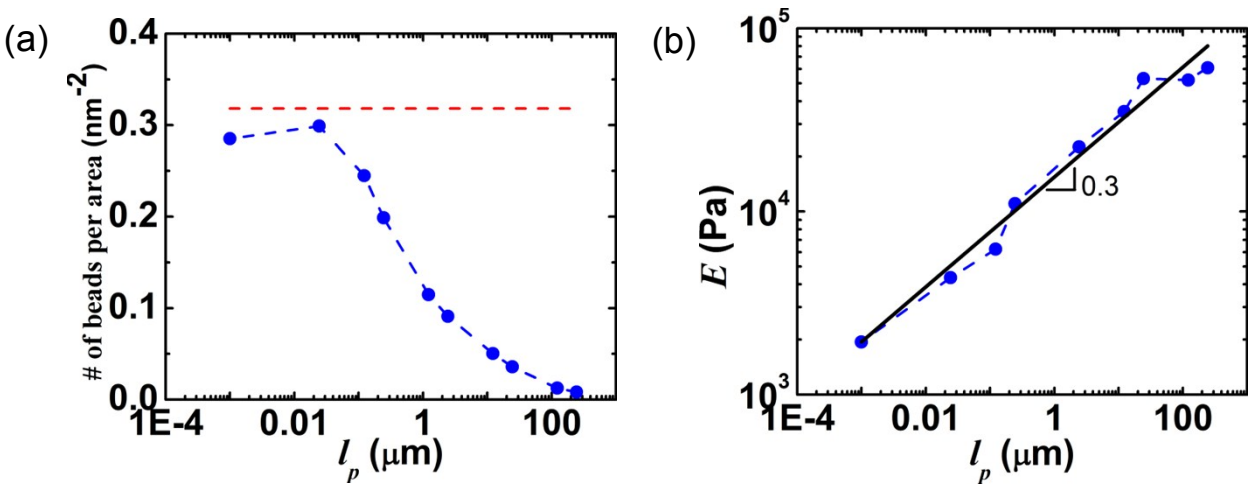

Figure S3. (a) The effect of fibril persistence length on the number of network beads in contact with the surface. The red line is the maximum number of beads per unit area (1/3.14 nm^{-2}), when network beads are tightly packed without gaps between them. (b) The effect of fibril persistence length on the Young's modulus of networks in the small strain range (secant slopes of curves in their linear regions of Figures S1a).

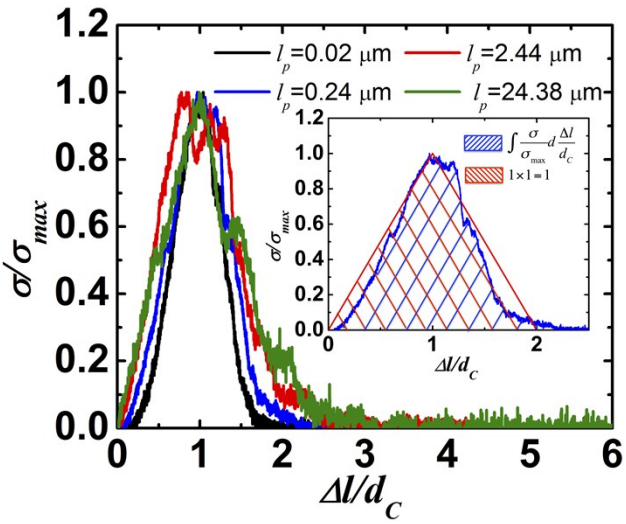

Figure S4. Plot of normalized stress vs. normalized displacement. Stress is normalized by the peak stress value attained, and displacement is normalized by its value corresponding to the peak stress The insert displays the estimation of area under the normalized stress-displacement curves as a triangle, which can be used as a simple cohesive law.

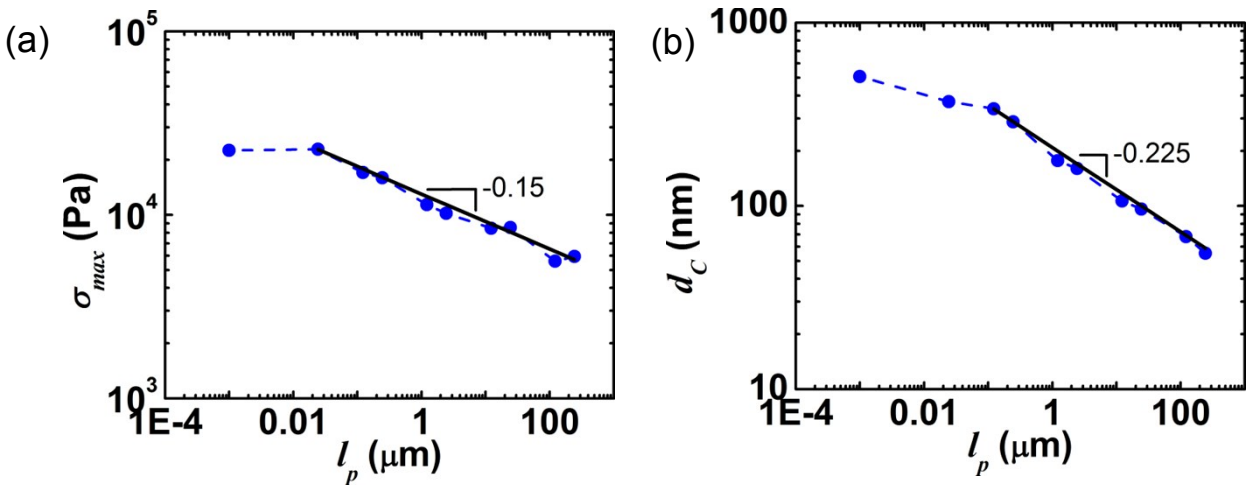

Figure S5. The effect of fibril persistence length on maximum stresses of networks and the corresponding displacements at maximum stresses during the desorption process.

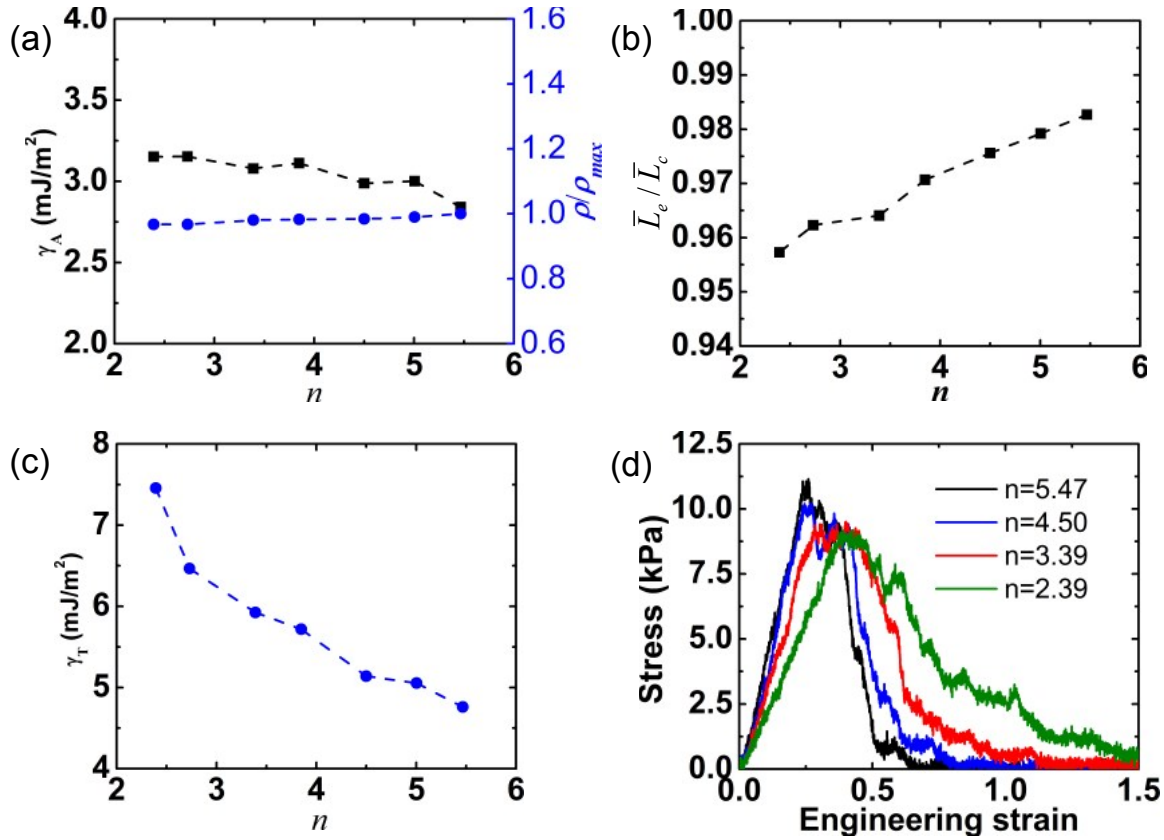

Figure S6. (a) The effect of crosslink density on the interfacial energy and network mass density; (b) The ratio of mean end-to-end distance ($\bar{L}_e$) to the mean contour length ($\bar{L}_c$) of fibril segments in networks with varying crosslink density; (c) The effect of crosslink density on the work of adhesion (γ_T); (d) The internal stress and strains generated in networks with different crosslink densities during the desorption process (l_p=2.44 μm and ε=1 k_BT).

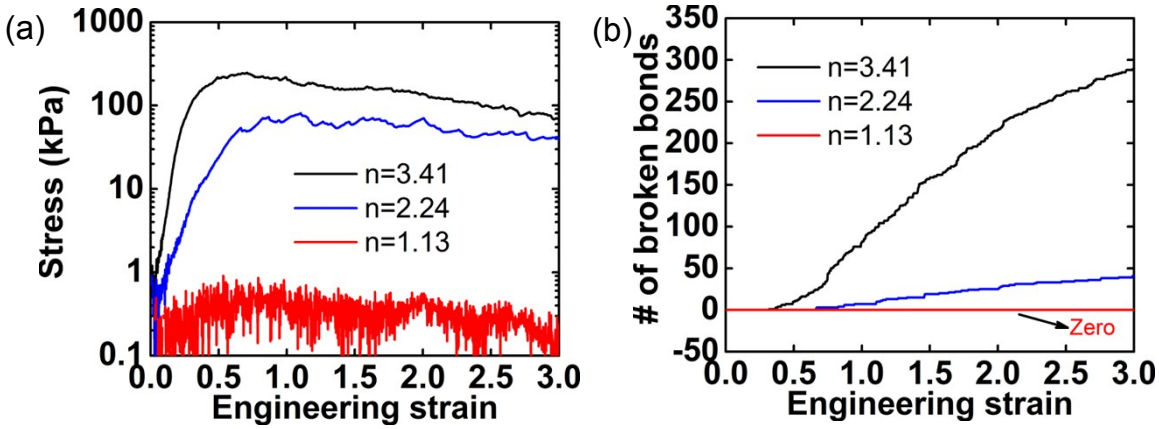

Figure S7. The stress generated (a) and the number of broken bonds (b) as a function of strain for three different crosslink densities and l_p=2.44 μm under tensile deformation. For networks with a higher crosslink density (n=2.24 and n=3.41), fibrils begin to rupture at large strains (>0.4), and the number of broken bonds increases with increasing strains. Fibril rupture and bond breaking are not observed in the fracture process of the network with a low crosslink density (n=1.13). Further simulations reveal a crosslink density threshold (n=1.56), below which networks fracture without fibril rupture. Instead, voids in these low-density networks coalesce to bigger voids until they percolate and span the cross-section at failure.